Two-photon Rabi oscillations

A. F. Linskens, I. Holleman, N. Dam,* and J. Reuss
Department of Molecular and Laser Physics, University of Nijmegen, Toernooiveld, NL-6525 ED Nijmegen, The Netherlands
(Received 2 May 1995; revised manuscript received 25 July 1996)

Rabi oscillations reflect the existence of a coherent superposition of two molecular eigenstates during the interaction of molecules with a strong, resonant electromagnetic field. This phenomenon is not restricted to two-level systems. We demonstrate its occurrence in a three-level system where the radiation induces a two-photon absorption. The intermediate level is (slightly) detuned from resonance. For a theoretical description the dressed-state picture is adopted. The two-photon excitation is performed either by using one laser, yielding a one-color two-photon process, or by using two counterpropagating, spatially overlapping laser beams, yielding a two-color two-photon process. Rabi oscillations are produced by varying the fluence, i.e., by changing either the laser power or the molecule-laser interaction time. For the one-color case the two-photon transition dipole moment for an SF_6 transition has been determined from the relation between laser fluence and number of Rabi oscillations. For the two-color cases the detuning with the intermediate level is varied by tuning the respective laser frequencies while keeping the sum frequency constant. A dramatic change in the degree of excitation as a function of the intermediate detuning has been observed. [S1050-2947(96)04712-9]

PACS number(s): 33.70.Ca, 42.65.Hw, 33.15.Mt

I. INTRODUCTION

The coupling between molecular eigenstates that is induced by a (near) resonant electromagnetic field can be described in terms of combined states of molecule and field (see, e.g., [1]). If a laser field is nearly resonant with a molecular transition the photon-induced coupling acts between doublets of these eigenstates. On resonance and in the limit of zero-field intensity these doublets become degenerate. For a nonzero field the degeneracy is lifted and the energy difference between the two doublet states linearly depends on the field amplitude.

Rabi oscillations reflect the (temporary) existence of a coherent superposition of the states making up a doublet. The superposition is created when a molecule enters the laser beam, and the contribution of each doublet state to the superposition depends on laser power and frequency. In the wave function describing the superposition state, the contributions from both molecular states evolve in time with an energy-dependent phase factor. On leaving the interaction zone the wave function is projected back onto the original doublet states. The resulting redistribution of initial population shows an oscillating behavior as a function of laser power, laser frequency, and interaction time.

Rabi oscillations on one-photon transitions in a two-level system have been measured in metastable Ne [2] and in SF_6 [3,4]. From the latter experiments the transition dipole moment of the fundamental ν_3 vibration has been extracted. In other experiments [5–7] the transition dipole moments were obtained for the ν_2 band of NH_3 and the ν_3 band of (di) fluoromethane using laser stark spectroscopy. In [7] the effects of a linear frequency sweep during the interaction time, by means of wave-front curvature or ac-Stark field inhomogeneity, which yield rapid passagelike effects, were investigated. In [8] microwave multiphoton Rabi oscillations between two Rydberg states in potassium are demonstrated and compared with Floquet theory.

These phenomena are not restricted to two-level systems but can be extended to multiphoton absorption schemes in which intermediate levels are involved. Here, laser radiation induces the absorption of two or more photons, the summed energy of which should equal the energy difference between the final and initial state of the multilevel system. The detuning of the field frequency with single photon transitions, involving the intermediate states, should be sufficiently small to enhance the transition probability significantly; but it also has to be sufficiently large to avoid populating intermediate states. If these special requirements are met any multilevel system can be reduced to an effective two-level system [9,10]. Calculations for the case of a resonant intermediate state have been presented by Shore and Ackerhalt [11] and Sargent and Morowitz [12].

Rabi oscillations on multiphoton transitions will be demonstrated here for a three-level system without relaxation under several experimental conditions. The simplest scheme consists of a one-color two-photon transition. The fluence can be varied by changing either the laser power or the size of the laser spot that determines the duration of the interaction time of the molecule in the laser field. Both techniques are applied and will be discussed. The analysis leads to a determination of the effective two-photon transition dipole moment for the $(v=0; J=4, E)\rightarrow(2\nu_3; J=3; E)$ transition in SF_6; E describes the rovibrational symmetry in the O_h-symmetry group.

II. THEORY

For the description of these phenomena the dressed-state picture [1,13] is used (see Fig. 1). The molecule is considered as submerged in a photon bath and the total energy of the molecule-photon system is considered. The possible energy states E_s of the isolated molecule are dressed by photon

*Author to whom correspondence should be addressed. Electronic address: nicod@sci.kun.nl

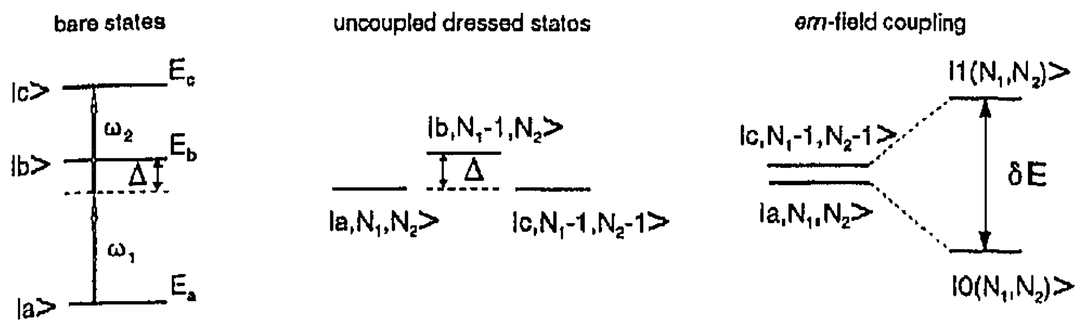

FIG. 1. Energy-level schemes of bare molecular states (left) and (uncoupled) dressed states (middle). The sum of the laser frequencies ω_1 and ω_2 is resonant with the transition $|a\rangle \rightarrow |c\rangle$. The intermediate detuning is denoted by Δ. The photon number states describing the laser fields are labeled by N_1 and N_2. At the right, the influence of radiative coupling of the otherwise degenerate doublet is shown. Note that actually $\delta E \ll \Delta$, so that the intermediate level does not have to be considered.

number states with energy $Nh\nu$ resulting in dressed-energy states $E^{\rm dr}_{s,N}$. The index $s=a,b,c$ labels the bare molecular states. In the case of two electromagnetic (em) fields with frequencies ν_1 and ν_2 this results in dressed-state energies $E^{\rm dr}_{s,N_1,N_2}=E_s+N_1h\nu_1+N_2h\nu_2$. For a three-level system with ground state $|a\rangle$, intermediate state $|b\rangle$, and final state $|c\rangle$ with energies E_a, E_b, and E_c, respectively, one obtains six nearly degenerate dressed states with energy (if at most two photons are exchanged)

$$E^{\rm dr}_{a,N_1,N_2}=E_a+N_1h\nu_1+N_2h\nu_2$$
$$\simeq\begin{cases}E_b+(N_1-1)h\nu_1+N_2h\nu_2\\ E_b+N_1h\nu_1+(N_2-1)h\nu_2\end{cases}$$
$$\simeq\begin{cases}E_c+(N_1-2)h\nu_1+N_2h\nu_2\\ E_c+(N_1-1)h\nu_1+(N_2-1)h\nu_2.\\ E_c+N_1h\nu_1+(N_2-2)h\nu_2\end{cases}$$

States which are off-resonant with respect to this multiplet are not taken into account; the assumption $E_b-E_a\approx E_c-E_b \approx h\nu_1\approx h\nu_2$ is made. The so-called uncoupled dressed states belonging to these dressed energies are written as $|a,N_1,N_2\rangle,|b,N_1-1,N_2\rangle$, etc.

The interaction of the molecule with the em field introduces a coupling between the uncoupled dressed states. In good approximation this coupling can be based on the electric dipole interaction $d_{ss'}\mathcal{E}_l$ between the electric field with amplitude $\mathcal{E}_l$ and the transition dipole moment $d_{ss'}$; the label $l=1,2$ distinguishes the different em field sources. The perturbation gives rise to off-diagonal elements in the Hamiltonian of the form $\hbar\Omega^l_{ss'}=d_{ss'}\mathcal{E}_l$ under the condition $N_1,N_2\gg 1$ (semiclassical limit). The perturbing term $\Omega^l_{ss'}$ is known as the Rabi frequency [14].

Choosing the energy of the dressed initial state as zero, $E^{\rm dr}_{a,N_1,N_2}=0$, the matrix Hamiltonian for a resonant two-color two-photon process involving two em field sources, $l=1,2$, can be approximated by

$$\mathcal{H}=\begin{pmatrix}0 & \frac{\hbar}{2}\Omega^{(1)}_{ab} & 0\\ \frac{\hbar}{2}\Omega^{(1)}_{ab} & 2\pi\Delta\hbar & \frac{\hbar}{2}\Omega^{(2)}_{bc}\\ 0 & \frac{\hbar}{2}\Omega^{(2)}_{bc} & 0\end{pmatrix}. \quad (1)$$

The detuning of the intermediate molecular state with the em field frequencies is here denoted by $h\Delta=(E_b-E_a-h\nu_1)=-(E_c-E_b-h\nu_2)$; the overall resonance condition for the sum frequency yields $(E_c-E_a)=h(\nu_1+\nu_2)$. In writing Eq. (1) we have assumed that $2\pi\Delta_1/\Omega^{(1)}_{ab}=(E_b-E_a-h\nu_1)/\hbar\Omega^{(1)}_{ab}\ll(E_b-E_a-h\nu_2)/\hbar\Omega^{(2)}_{ab}=2\pi\Delta_2/\Omega^{(2)}_{ab}$, so that the other two-photon absorption pathway can be neglected (see also Sec. IV B below). This elementary matrix operator then describes the interaction for the near resonant case, if the intermediate detunings $|\Delta_l|$ are sufficiently large. In Fig. 1 the energy-level schemes for the bare molecular model and the dressed model are shown, together with the influence of dipole coupling of the two otherwise degenerate levels, $|a,N_1,N_2\rangle$ and $|c,N_1-1,N_2-1\rangle$. The corresponding coupled dressed eigenstates, that is, eigenstates of $\mathcal{H}$ in Eq. (1), are denoted by $|0(N_1,N_2)\rangle$ and $|1(N_1,N_2)\rangle$.

A. Rabi oscillations in a three-level system

The population of molecular field-free eigenstates changes if these states are coupled by laser photons. In the three-level system described here the three molecular eigenstates that participate are $|a\rangle$, $|b\rangle$, and $|c\rangle$, with an initial population of 100% in $|a\rangle$. As a result of the interaction between the molecule and the em field the degeneracy of the uncoupled dressed doublet is lifted and the new coupled dressed eigenstates are separated in energy by δE, see Fig. 1. If the em field is switched on suddenly, a molecule initially in $|a\rangle$ is found in a state that is a coherent superposition of $|0(N_1,N_2)\rangle$ and $|1(N_1,N_2)\rangle$, the latter being the appropriate eigenstates in the presence of the field. The contributions of both these new eigenstates evolve in time with their own, energy-dependent, phase factor. On leaving the em field the superposition state is projected back onto the field-free molecular states leading to a population distribution that depends in an oscillatory way on the duration and strength of the interaction.

To obtain a "clean" two-photon Rabi oscillation between $|a\rangle$ and $|c\rangle$ the intermediate state $|b\rangle$ should not acquire significant population. The intermediate detuning $|\Delta|$ should thus be large compared to the one-photon Rabi frequencies $\Omega^{(1)}_{ab}$ and $\Omega^{(2)}_{bc}$. On the other hand, the detuning should be small enough to provide for sufficient two-photon transition strength.

Diagonalizing the Hamiltonian of Eq. (1) for the three-level system under this condition, $2\pi|\Delta|\gg\Omega^{(1)}_{ab},\Omega^{(2)}_{bc}$, yields an analytical expression for the energy difference between the states $|0(N_1N_2)\rangle$ and $|1(N_1N_2)\rangle$ [9,15–17],

$$\delta E=\hbar\Omega \quad \text{with} \quad \Omega=\sqrt{\Omega^2_{ac}+\delta\omega^2} \quad \text{with} \quad \Omega_{ac}=\frac{\Omega^{(1)}_{ab}\Omega^{(2)}_{bc}}{4\pi\Delta}. \quad (2)$$

Here Ω is the generalized Rabi frequency, Ω_{ac} is the two-photon Rabi frequency, and $\delta\omega$ a possible small detuning of the sum frequency $2\pi(\nu_1+\nu_2)$ from the frequency where the transition probability assumes a maximum value (taking into account ac-Stark shifts [16,18]).

In case of a large detuning, $\Delta\gg\delta E$, the three-level system thus reduces effectively to a two-level system. The population then oscillates between states $|a\rangle$ and $|c\rangle$ with the generalized Rabi frequency Ω. It can also be expressed analyti-

cally as a function of the laser-molecule interaction time τ and the two-photon Rabi frequency Ω_{ac},

$$\rho_{cc}=\frac{\Omega_{ac}}{\sqrt{\Omega_{ac}^2+\delta\omega^2}}\sin^2\left(\frac{\sqrt{\Omega_{ac}^2+\delta\omega^2}}{2}\tau\right). \quad (3)$$

Here, ρ_{cc} stands for the fractional population of $|c\rangle$, with $\rho_{aa}+\rho_{cc}=1$ and $\rho_{bb}=0$. The excitation amplitude (factor in front of the $\sin^2$) is a function of the two-photon Rabi frequency and determines the maximum degree of excitation. In case of exact two-photon resonance ($\delta\omega=0$) Eq. (3) reduces to

$$\rho_{cc}=\sin^2\left(\frac{\Omega_{ac}\tau}{2}\right). \quad (4)$$

The effective interaction time τ_{eff} in the case of a two-photon interaction involving a Gaussian laser profile follows from the pulse-area theorem [19] (see the Appendix),

$$\tau_{\text{eff}}=\sqrt{\pi/2}\,\frac{w_0}{v} \quad (5)$$

with w_0 the laser waist radius and v the velocity of the molecule. If we count subsequent extrema in ρ_{cc} by an index number n, that is,

$$n=\frac{\Omega_{ac}\tau_{\text{eff}}}{2\pi}, \quad (6)$$

maxima and minima in ρ_{cc} are found for $n=1,3,5,\ldots$ and $n=2,4,6,\ldots$, respectively. Note that for the case of a one-color ($\mathcal{E}_1=\mathcal{E}_2$) two-photon transition $\Omega_{ac}\tau\propto P/w_0$, whereas for a one-photon transition $\Omega_{ab}\tau\propto\sqrt{P}$, *see Eq.* (2)

III. EXPERIMENT

The prototype three-level system used for the experiments consists of the $P(4)E$ rovibrational two-photon transition of the vibrational ν_3-ladder in SF_6. The two-photon resonance frequency is +348 MHz detuned with respect to twice the fundamental frequency of the 10P16 CO_2 laser line center [20,21]. The single intermediate level involved is detuned by +250 MHz from the same laser line [22]. The two-photon transition can be induced by either a single-laser interacting with the molecules or by two simultaneously interacting laser fields. Both types of two-photon excitation processes will be discussed. For the single-laser interaction the two-photon transition is denoted as ''one-color two-photon'' transition and the resonance frequency is +174 MHz detuned to the blue with respect to the 10P16 CO_2 laser line. A two-laser interaction yields a ''two-color two-photon'' transition. In practice this means that both lasers are set to the 10P16 CO_2 laser line center with a sum detuning of +348 MHz.

The experimental setup has been described earlier in [13,20,21,23]. It consists of two high-power, single-frequency CO_2 waveguide lasers and a molecular-beam apparatus that provides a large population of the $J=4$ rotational state in the vibrational ground state of SF_6. The used laser system consists of two CO_2 waveguide lasers locked to Fabry-Pérot étalons. The lasers are stable in frequency with a short-term fluctuation of $\ll$10 kHz. The long-term drift could be minimized to several 100 kHz in 10 min. This suffices to keep the lasers in resonance with the molecular transition frequency during the experiments with a typical recording time of 1–2 min. The power stability of the lasers was better than 1%. The laser beams together with the molecular beam span a horizontal plane.

To tune the laser frequency into resonance with the two-photon transition use was made of optoacoustic modulators (OAM, IntrAction Corp.). These modulators shift the laser frequency by 100 MHz per pass through the crystals. The laser power is reduced by about a factor of 2 on each pass. Together with the tuning range of the lasers themselves of more than 100 MHz to both sides of the line center, the maximum achievable detuning from the central laser frequency amounts to $\pm$300 MHz for both lasers, the laser beams passing twice through the OAM.

The intensity of the frequency-shifted laser beam can be controlled by adjusting the diffraction efficiency of the OAM, which depends on the rf power fed into the crystal. Care was taken to avoid beam deflection that might be caused by this way of varying the laser intensity.

A stringent condition for producing Rabi oscillations with high contrast is to avoid rapid adiabatic passage (RAP) phenomena which, in our case, are mainly caused by the curvature of the laser-field wave fronts [20,24,25]. The effects of wave-front curvature can be minimized by using a telescope to suppress beam divergence [26]. Additionally, the focus of the laser beam should coincide precisely with the interaction region with the molecular beam.

For the telescope an $f=25$ cm in combination with an $f=40$ cm lens is used producing a laser waist $w_0=4.0$ mm at a distance of 6 m. Alternatively, ''sharp focusing'' [20] could be realized with lenses of $f=20$ cm producing a laser waist of $w_0=0.25$ mm at the laser-molecules interaction region. This technique, however, produces flat wave fronts only near the molecular beam axis (waist length only 20 mm), whereas the outer parts of the molecular beam (that still reach the detector) experience already nonnegligible wave-front curvature.

Both optical systems (telescope and sharply focused) have been applied, utilizing the experimental setup shown in Fig. 2; SF_6 was seeded in He (2%) and expanded through a 30-μm nozzle with a stagnation pressure of 2 bars at room temperature. The velocity of the beam molecules is 1250 m/s. The detection of the change in internal energy of the beam molecules was performed with a liquid-He-cooled bolometer ($\simeq$1.5 K) applying lock-in techniques [27]. The bolometer dimensions are 5 mm (horizontal)$\times$1 mm (vertical). To obtain circularly polarized light a $\frac{1}{4}\lambda$ plate was inserted in the laser beam; no distinction has been made between left- and right-handed polarization. All data acquisition took place by computer.

IV. RESULTS

A. One-color excitation

Two-photon Rabi oscillations with one laser focused to a diameter of $2w_0=0.5$ mm were obtained by recording the excited-state population as a function of the laser power (''power scan''). The results are shown in Fig. 3(a). The

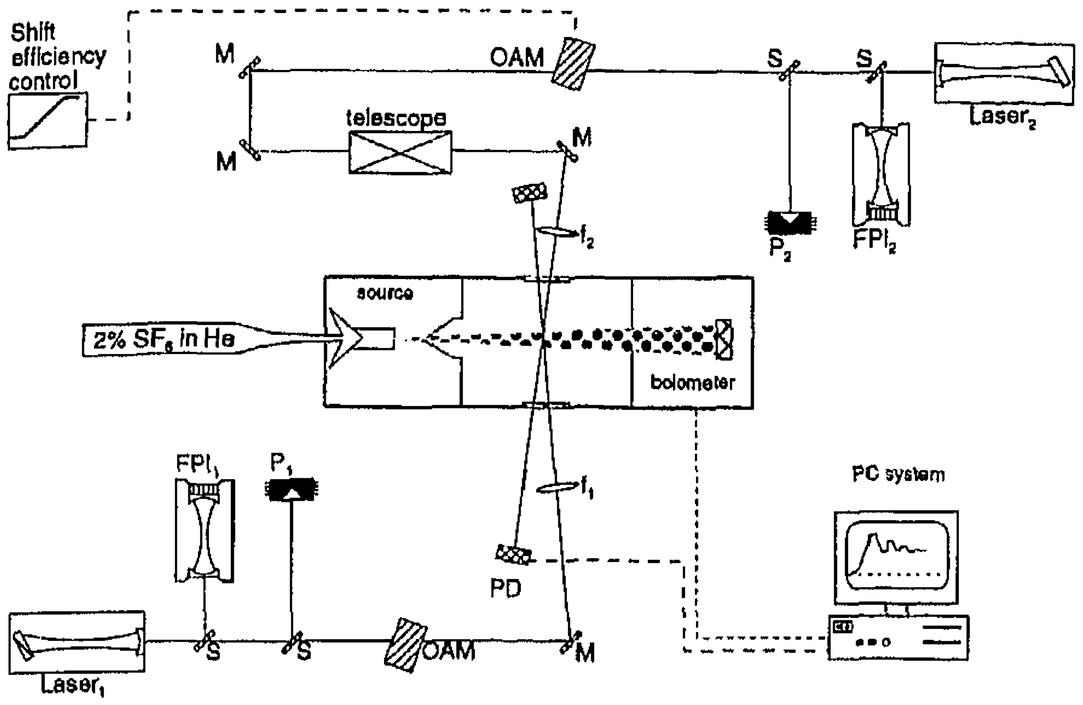

FIG. 2. The experimental setup consists of two laser systems interacting with molecules in a skimmed molecular beam. The lasers, étalons, power meters, and lenses are denoted by L_i, FPI_i, P_i, and f_i, respectively. Further, M is the mirror, S is the beam splitter, and OAM is the optoacoustic modulator. PD stands for the pyrodetector used to record the laser power simultaneously with the bolometer signal.

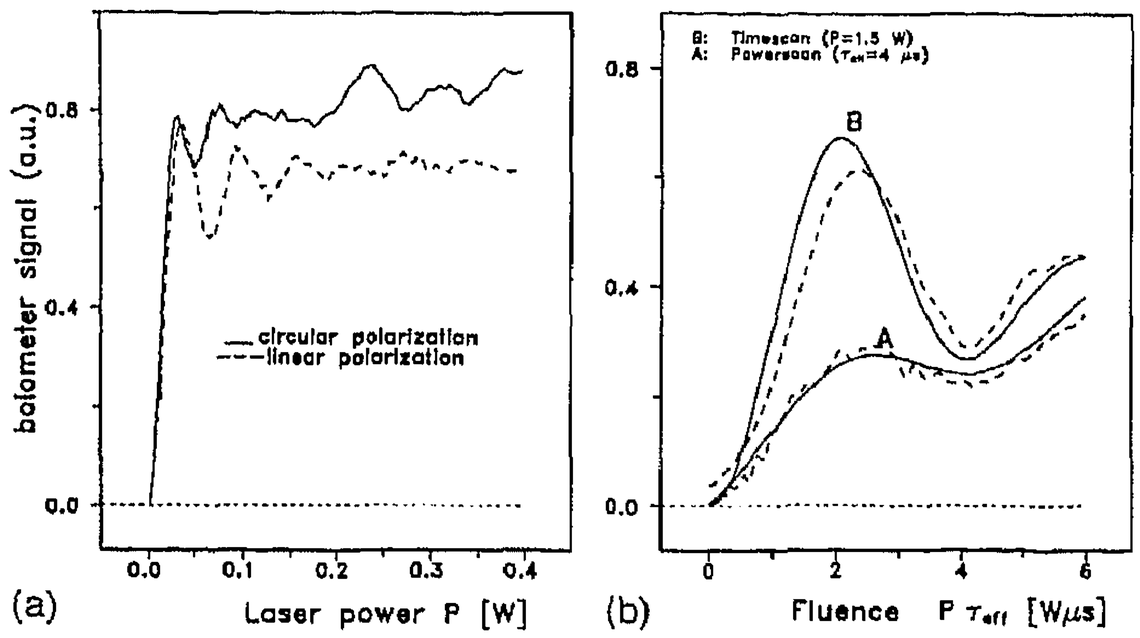

FIG. 3. (a) shows the one-color two-photon Rabi oscillations for linear (dashed trace) and circular (solid trace) laser field polarization, for increasing power P and an interaction length of 0.5 mm. The vertical scale shows the bolometer signal; a value of 1.0 corresponds to complete inversion. (b) shows the Rabi oscillations of a varied interaction length of up to 8 mm, corresponding to an effective interaction time $\tau_{\text{eff}}=4.0$ μs. [Calculated from the slit width $2a$, using Eq. (A3).] For trace B the power was kept fixed at 1.5 W and the interaction time was changed from 0 to 4.0 μs. For trace A the interaction time was kept fixed and the laser power was changed from 0 to 1.5 W. The solid traces represent simulations.

dashed trace shows the oscillations for a linearly polarized laser field and the solid trace for a circularly polarized laser field.

The contrast between the maxima and minima in the signal is affected by two different phenomena: first, the M dependence of the transition dipole moments d_{ab} and d_{bc}, where M denotes the quantum number corresponding to the projection of the angular momentum on a space fixed axis (determined by the laser polarization). The Rabi frequency depends on $|M|$ and the observed signal stems from the superimposed contributions of different M values. With increasing laser power the smearing out of different Rabi frequencies becomes more pronounced resulting in a reduced contrast. The trace for linearly polarized light shows a contrast of 25%. The maximum signal is obtained for $n=1$ [Eq. (6)]. For circularly polarized light the contrast vanishes faster, indicating a larger spread in the M-dependent Rabi frequencies. The sharp focus introduces RAP effects in the outer parts of the molecular beam. Since rapid adiabatic passage produces transitions without Rabi oscillations, this reduces the contrast in the oscillations observed, as discussed in [7].

With the extended laser beam diameter of 8 mm Rabi oscillations were produced by changing the laser power as well as the interaction time. The latter was achieved by placing a horizontal slit with adjustable width into the laser beam. By changing the slit width the interaction time of the molecules with the laser field is varied. The results are shown in Fig. 3(b). Trace B shows the result for increasing interaction time for a fixed (relatively high) power of 1.5 W. Trace A shows the result for increasing power with a fixed laser beam diameter of 8 mm. The product of laser power and interaction time (i.e., the fluence) is plotted on the abscissa; this parameter is varied in both scan types. Since the excited-state population is a function of fluence only [Eq. (4)], the power scan and the interaction-time scan should produce similar results. The solid traces represent simulations, discussed below.

The large difference in contrast between both recording techniques is caused by the Doppler residue ($|\delta\nu_D|\simeq 400$ kHz) of the molecular beam determined by the detector size (5 mm). In case of the 8-mm interaction length (trace A) the first π pulse is obtained for a two-photon Rabi frequency of 100 kHz. From Eq. (3) it is seen that a local detuning of $\delta\omega_D=2\pi\delta\nu_D$ reduces both the Rabi-oscillation amplitude and its oscillation period, if it becomes nonnegligible with respect to $|\Omega_{ac}|$.

For a fixed laser power of 1.5 W and a changing slit width the first π pulse is observed for a slit width of 3 mm (trace B). The influence of the Doppler residue is three times smaller here and the contrast is strongly enhanced.

The number of π pulses, n of Eq. (6), is plotted in Fig. 4 as a function of increasing laser power for the linearly polarized laser beam, with interaction lengths of 0.5 and 8 mm and for the circularly polarized laser beam with an interaction length of 0.5 mm. The straight lines are linear fits through the data points. The slopes (n over laser power P) are proportional to $d_{ab}d_{bc}/(w_0\Delta)$ [see Eqs. (2) and (6)]. For the linearly polarized beam, the slope for the $2w_0=8$ mm case can be scaled to the $2w_0=0.5$ mm case through multiplication by a factor of 16. Rescaling the experimental value of 1.8 W^{-1} (□ of Fig. 4) one obtains 29 W^{-1}, which is in satisfactory agreement with the experimental value of 32 W^{-1} (△ of Fig. 4).

B. Two-color excitation

If two (counterpropagating) lasers with different frequencies are used, the laser powers and the detuning of the laser frequencies with respect to the intermediate level can be chosen independently. To perform the experiments the laser fields are made to interact simultaneously with the molecular beam. Both lasers are focused with an $f=20$ cm lens to a

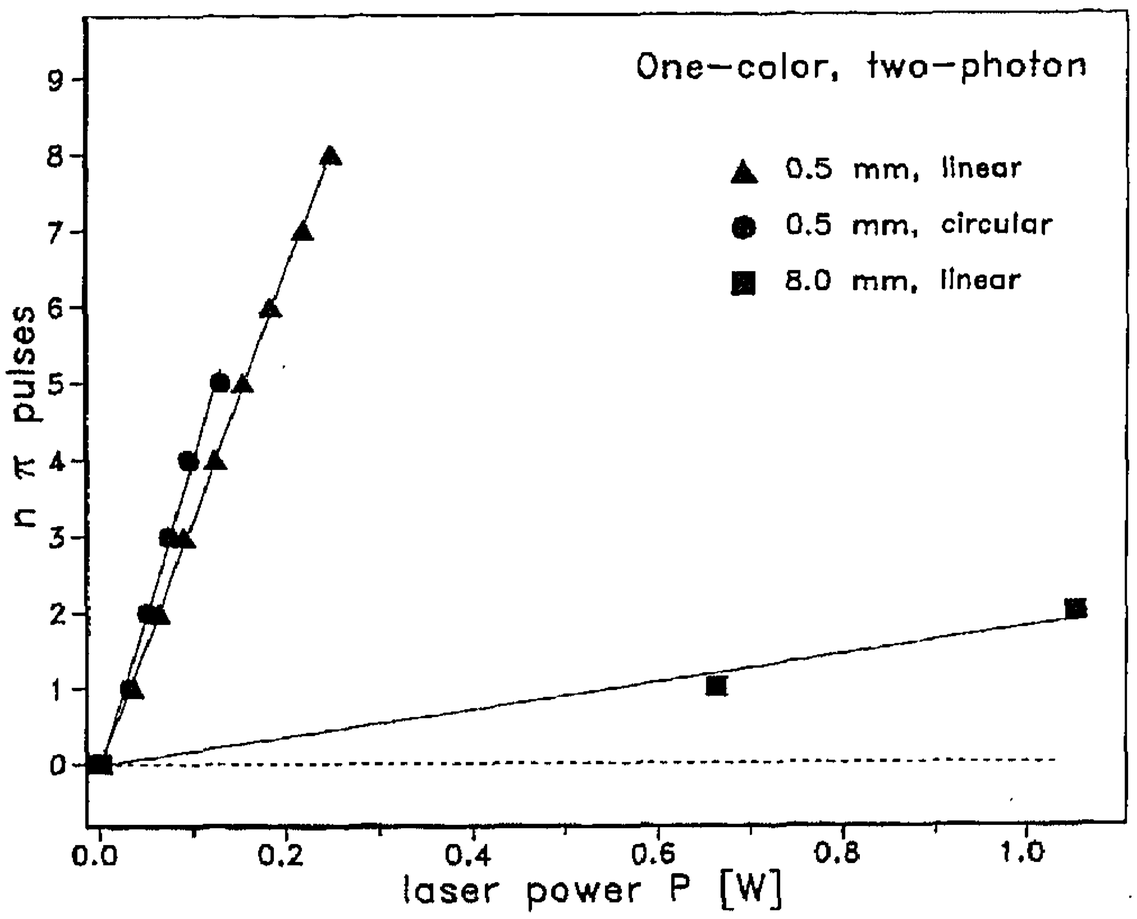

FIG. 4. The number n of π pulses for increasing laser power obtained from Figs. 3(a) and 3(b). The symbols △, ○, and □ correspond to a 0.5-mm-diam focus with linearly and circularly polarized light and to an 8-mm focus with linear polarized light, respectively. The respective slopes are 32, 40, and 1.8 W^{-1}.

waist diameter of $2w_0=0.5$ mm. The foci are aligned such that with each individual laser one-color two-photon Rabi oscillations are observed.

Accurate alignment is achieved by horizontally translating the focus of laser 1 along the molecular beam, through the focus of laser 2. Both laser intensities are kept below saturation of the two-photon transition. In this case the two-color two-photon signal depends strongly on the overlap of both laser beams, as illustrated in Fig. 5(b). The used laser power is 10 mW for both lasers. The laser beams cross under a small angle to avoid mutual perturbations.

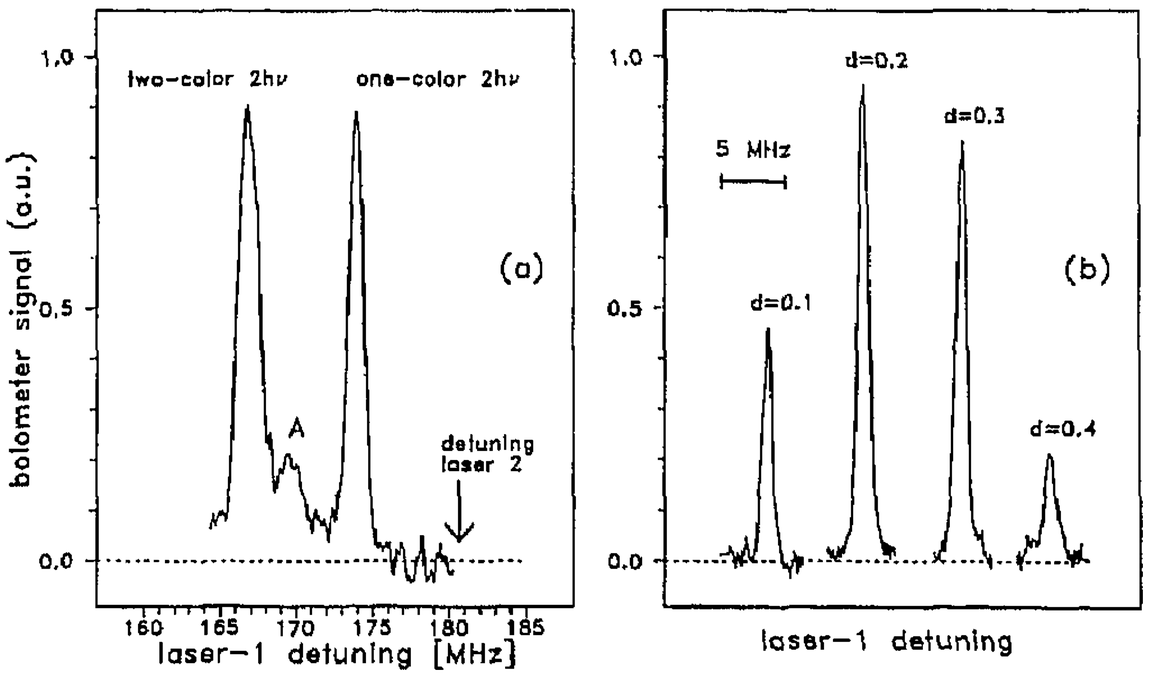

FIG. 5. (a) shows the one-color two-photon signal for a detuning of laser 1 from the $10P16$ CO_2 line center of 174 MHz and the two-color two-photon signal for laser 1 at 167 MHz. Laser 1 is tuned in frequency and laser 2 is kept fixed in frequency at 181 MHz (arrow). The peak indicated by A is an unimportant weak two-color feature. (b) shows the line profile of the two-color two-photon resonance for different relative laser focus positions d (in mm, with arbitrary offset), at low-laser intensities, $n \ll 1$. The signal strength is seen to respond sensitively to displacements as small as 0.1 mm.

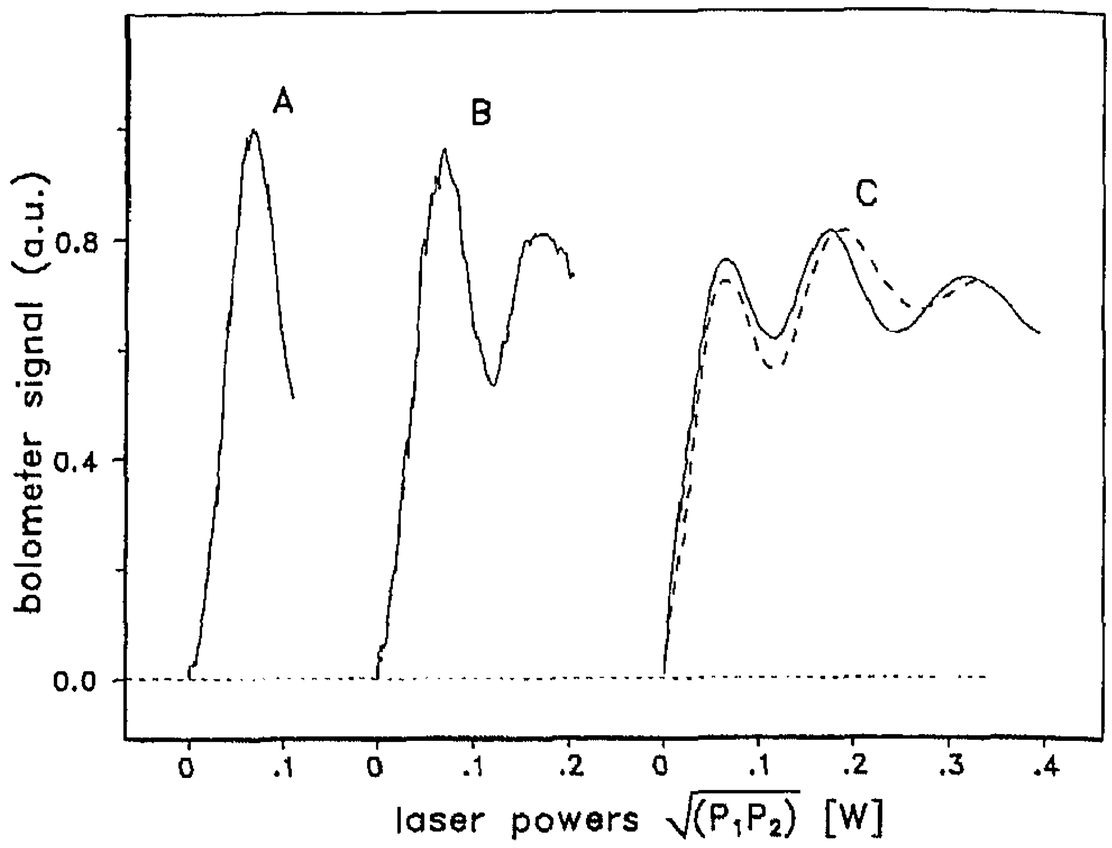

FIG. 6. Two-color two-photon Rabi oscillations for fixed values of the power of laser 2, viz., 20 mW (trace A), 50 mW (trace B), and 300 mW (trace C), and increasing power from 0 to 1.0 W of laser 1. Note the decrease in contrast with increasing laser 2 power. In trace C the difference between solid and dashed curves results from the interchange of laser 1 and laser 2. The detuning of the intermediate level equals $\Delta_1=55$ MHz and $\Delta_2=97$ MHz for either ν_1 or ν_2 being absorbed in the first step, respectively.

To obtain the two-color two-photon signal laser 2 is kept fixed in frequency, slightly detuned to the blue with respect to the one-color two-photon resonance. The bolometer signal (i.e., the excited-state population) is recorded as a function of the frequency of laser 1; both one-color and two-color resonances occur, see Fig. 5(a). The used laser power of 10 mW corresponds to $\Omega/2\pi=0.8$ MHz and $\Omega\tau_{\text{eff}}=0.3\pi$. Instead of the expected Doppler-free two-color signal for the two counterpropagating laser beams, a broadening by about a factor of 2 is observed (as compared to the one-color transition). This is due to the fact that, in addition to the interaction time broadening (which amounts to 2 MHz for the sharp foci), laser 2 gives rise to M-level splitting (induced by the ac-Stark effect) which is also probed by laser 1. This phenomenon is absent in the case of the one-color two-photon transition. Note that the use of two overlapping but counterpropagating waves eliminates RAP effects.

Two-photon two-color Rabi oscillations were produced by increasing the power of laser 1 with fixed power of laser 2. The lasers are tuned to a frequency of 195 MHz (laser 1) and 153 MHz (laser 2) with respect to the $10P16$- CO_2 laser line. The intermediate detunings amount to $\Delta_1=55$ MHz and $\Delta_2=97$ MHz, respectively. The results are shown in Fig. 6 for fixed power of laser 2 of 20 mW (trace A) and 50 mW (trace B); the power of laser 1 is varied up to 1 W. Trace C shows the result of interchanging the lasers; the power of either laser 1 or laser 2 is varied, whereas the other is kept fixed at 300 mW. The similarity of the solid and dashed traces proves that both lasers couple to the molecules in nearly identical ways.

On increasing the power of the fixed-power laser the contrast in signal is reduced, from >50% (trace A) to 20% (trace C). This is explained by an increased M-level splitting, caused by the stronger laser. In addition, the two-color two-photon process actually involves two different pathways. If

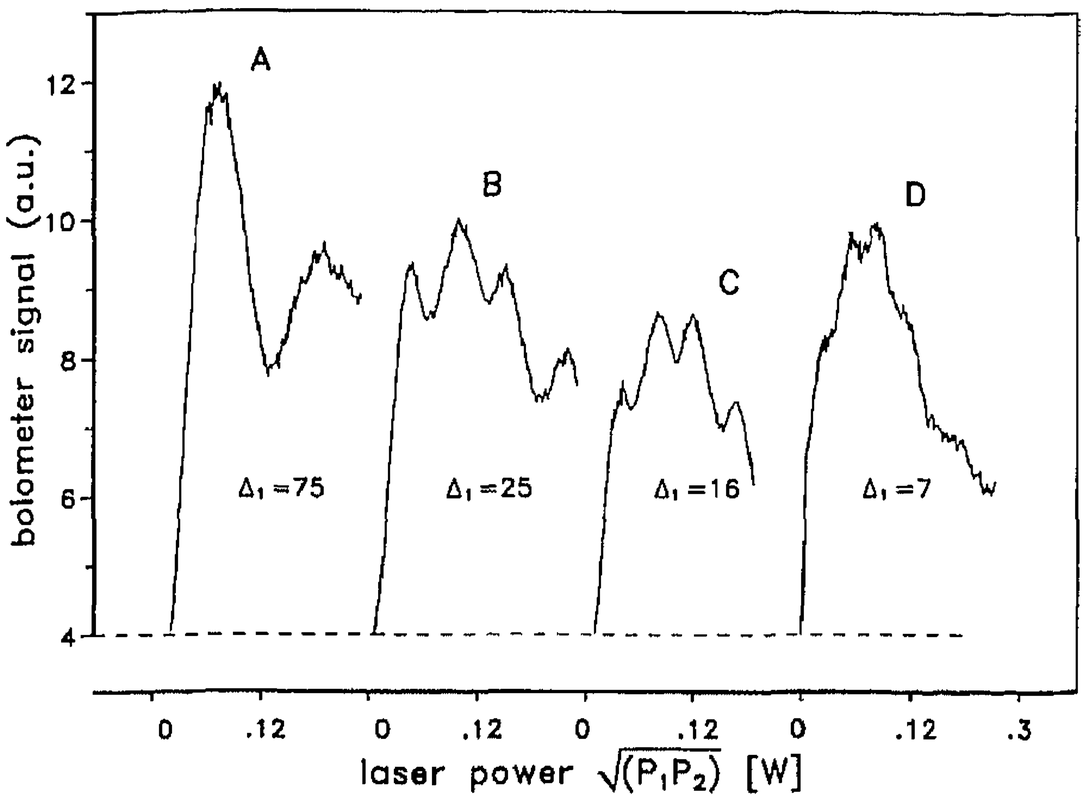

FIG. 7. Two-color two-photon Rabi oscillations obtained for various values of the intermediate detuning Δ_1. The intermediate detuning was varied while keeping the sum frequency on resonance. The traces correspond to $\Delta_1=70$ MHz (trace A), $\Delta_1=25$ MHz (trace B), $\Delta_1=16$ MHz (trace C), and $\Delta_1=7$ MHz (trace D). The Rabi oscillations are obtained with the power of laser 2 fixed at 200 mW; the power of laser 1 is changed from 0 to 300 mW.

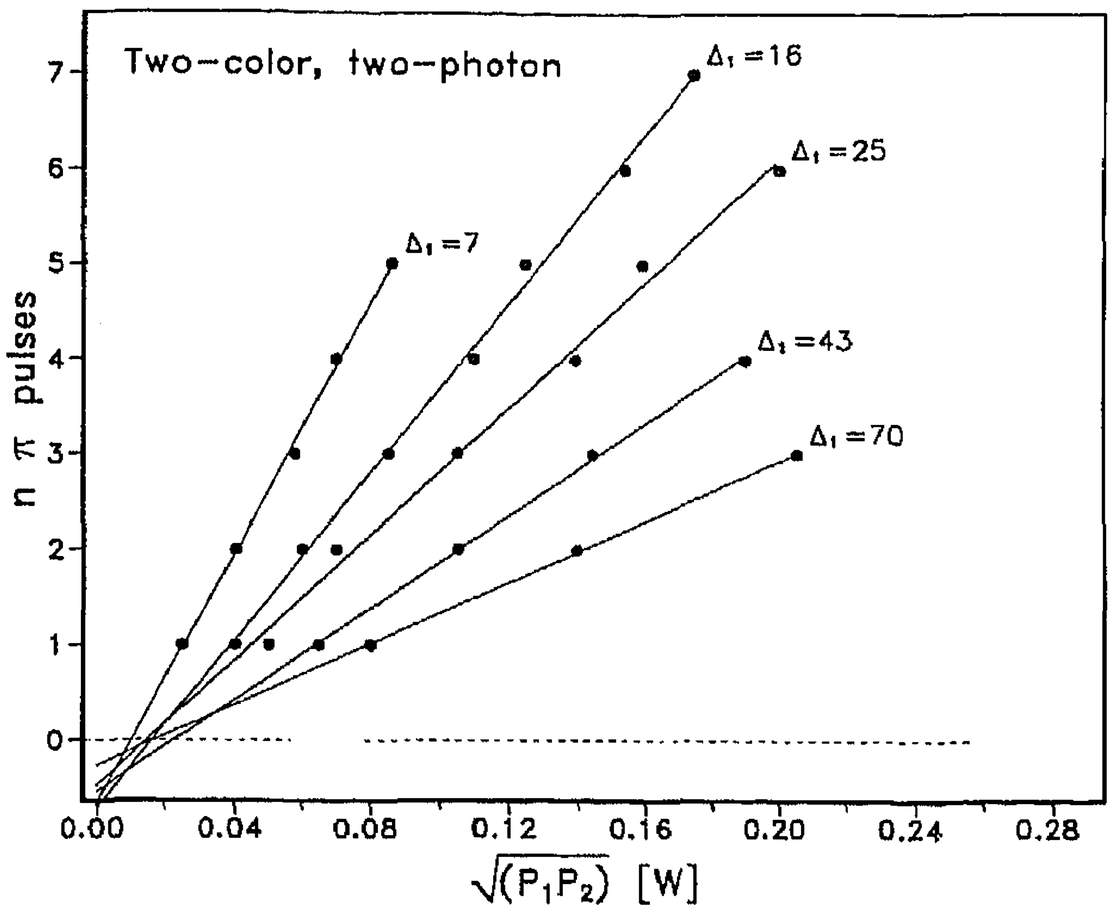

FIG. 8. The number of n of π pulses obtained for the various intermediate detunings (Fig. 7) indicated by Δ_1 (in MHz) for increasing laser power $\sqrt{P_1P_2}$.

the two photons are denoted by ν_1 and ν_2 a two-photon transition can proceed either by absorbing first a photon ν_1 followed by ν_2 or vice versa. Both pathways are associated with different intermediate detunings, viz., $\Delta_1=\nu-\nu_1$ or $\Delta_2=\nu-\nu_2$ (ν being the one-photon transition frequency) and therefore with different Rabi frequencies. Their interference gives rise to a reduced contrast.

In Fig. 6 the relative amplitudes for $n=1,3,5,\ldots$ are seen to decrease with increasing power of laser 2. At the same time, the number of Rabi oscillations increases.

To investigate the role of the intermediate detuning, power scans at different values of Δ_1 were made. For various intermediate detunings the Rabi oscillations are obtained by varying the power of laser 1 for a fixed value of the power of laser 2. The results for intermediate detunings Δ_1 equal to 70, 25, 16, and 7 MHz (corresponding values for Δ_2 are 278, 323, 332, and 341 MHz, respectively) are shown in Fig. 7, trace A, B, C, and D, respectively. For decreasing Δ_1 the observed Rabi oscillations are seen to become more closely spaced and finally are barely resolvable any more (trace D).

The number n of π pulses is plotted in Fig. 8 as a function of $\sqrt{P_1P_2}$. Comparison of Fig. 8 with Fig. 4 shows that—for given Δ_1—the measured points scatter considerably around a straight line fitted through the data points. This scattering is absent in Fig. 4. In addition the linear fit goes only approximately through the origin. The slopes of the linear fits are expected to be proportional to $1/\Delta_1$, see Eqs. (2) and (6). In Fig. 8, however, for the detunings $\Delta_1=7$ and 70 MHz, the slopes s obey the relation $s(\Delta_1=7)\approx 3.8s(\Delta_1=70)$.

V. DISCUSSION

For a nearly equidistant three-level system $|a\rangle$, $|b\rangle$, and $|c\rangle$ one-color and two-color Rabi oscillations have been observed between $|a\rangle$ and $|c\rangle$, with $\Omega_{ac}/2\pi$ typically in the range of 2.5 MHz($n=1$)–25 MHz($n=10$). After the laser interaction, the molecular state is described by

$$\alpha \exp^{-iE_at/\hbar}|a\rangle+\gamma \exp^{-iE_ct/\hbar}|c\rangle. \tag{7}$$

The bolometer signal is proportional to $|\gamma|^2$. The coefficients α and γ depend on the product $\Omega_{ac}\tau_{\text{eff}}$. The amplitudes $|\alpha|$ and $|\gamma|$ assume maximum (minimum) values for $n=1,3,5,\ldots$ ($n=2,4,6,\ldots$) if

$$\frac{1}{2\pi\Delta_1}\frac{\sqrt{P_1P_2}}{\pi\epsilon_0 c w_0^2}\frac{d_{ab}d_{bc}}{\hbar^2}\frac{xw_0}{v}=n\pi, \tag{8}$$

with $x=\sqrt{\pi/2}$ (see the Appendix). In Eq. (8), perfect coincidence of two Gaussian laser waists is assumed, $w_1=w_2=w_0$. In the case of nonlinear one-color interaction, $P_1=P_2$ and $\Delta_1=\Delta$. For the two-color interactions, only the pathway with ν_1 absorption as the first step is taken into account. Rewriting Eq. (8) one obtains a relation between $d_{ab}d_{bc}$ and the measured slopes (Figs. 4 and 8),

$$d_{ab}d_{bc}=2\pi\Delta_1\frac{\epsilon_0 c v w_0 h^2}{4x}\frac{n}{\sqrt{P_1P_2}}. \tag{9}$$

For the one-color measurements the effective value for $d_{ab}d_{bc}$ obtained from the linear fit under different experimental conditions is listed in Table I.

For the ν_3 ladder of SF_6, $d_{ab}d_{bc}$ can be calculated for the two successive one-photon steps, including the contributions of specific M values,

$$d_{ab}d_{bc}=d_0^2 f\sqrt{2J_b+1}\begin{pmatrix} J_a & 1 & J_b \\ -M_a & \mu & M_b\end{pmatrix} \times\sqrt{2J_c+1}\begin{pmatrix} J_b & 1 & J_c \\ -M_b & \mu & M_c\end{pmatrix}. \tag{10}$$

Equation (10), including the factor $f=0.735$, is derived in [28] for the vibrational excitation of two mutually perpendicular oscillations and includes the first-order Coriolis correction term for this specific type of excitation. The rota-

TABLE I. Values for the effective dipole moment $d_{ab}d_{bc}$ and the resultant transition dipole strength d_0 for different experimental conditions. Columns 1–3 characterize the experiment. Column 4 gives the "slopes" as obtained from the linear fits in Fig. 4. The values for d_0 in column 5 should be compared with the theoretical value of d_0=0.437 D.

Polarization	w_0 (mm)	Δ (MHz)	slope (W^{-1})	$d_{ab}d_{bc}$ (D^2)	d_0 (D)
linear	0.25	76	32.2	0.0503	0.44(4)
linear	4.0	76	1.77	0.0459	0.42(4)
circular	0.25	76	40.0	0.0629	0.43(4)

tional quantum numbers $J_{a,b,c}$ of the three successive states involved are J_a=4, J_b=J_c=3. In the case of two parallel linearly polarized photons we have μ=0; for circular polarization μ=1. The value of $d_{ab}d_{bc}$ for different M_a, M_b, and M_c calculated from Eq. (10) are listed in Table II, for linearly and circularly polarized light.

In the measurements the sum of contributions of all M_a sublevels is observed. The laser intensity for which maxima and minima occur is determined by the strongest M contributions. The weaker M components give rise mainly to a reduction of contrast and a slight shift in the position of the minima and maxima. From Table II it is seen that for linearly polarized light mainly the transitions with $|M_a|$=2 and 3 contribute to $d_{ab}d_{bc}$; for circularly polarized light the main contributions arise from the M_a sublevels with $|M_a|$=4, 3, and 2. The average main value (a.m.v) for those sublevels from which the resulting dipole strength is estimated are listed in column three.

With this averaged main value the dipole strength d_0 is calculated, see Table I in good agreement with the generally accepted value of d_0=0.437 D [29]. The uncertainty of 10% in the experimental value stems mainly from the not-precisely-known velocity of the beam molecules (1250±100 m/s). The value for the laser waist diameter is calculated using Gaussian beam formulas; the uncertainty in this parameter amounts to 5%. The value of the laser power is known with an accuracy of 5%. The intermediate detuning Δ is known precisely for the one-color two-photon transition (76 MHz).

TABLE II. In the first column the initial M_a values are specified. In the second column the values of $d_{ab}d_{bc}$ are listed obtained in terms of d_0 [Eq. (10)]. The average mean value (a.m.v.) of the strongest contributions is given in column 3.

Linear polarization, $\|\Delta M\|$=0		
$\|M_a\|$	$d_{ab}d_{bc}$	a.m.v.
0		
1	0.14	
2	0.24	0.26
3	0.28	

Circular polarization, ΔM=−1		
M_a	$d_{ab}d_{bc}$	a.m.v.
−1	0.11	
0	0.19	
1	0.27	
2	0.34	
3	0.36	0.34
4	0.32	

For the linearly polarized laser beam with a diameter of 8 mm simulations of the power scan and the time scan have been performed, based on the optical Bloch equations [14,19]. The total population in the final state, ρ_{cc}^{tot} has been calculated as a function of the fluence σ taking into account the M dependence of $d_{ab}d_{bc}$, that is,

$$\rho_{cc}^{\text{tot}}(\sigma)=\int_{\delta\nu_D}\sum_{M=-4}^{+4}\rho_{cc}^{M}(\sigma), \tag{11}$$

with $\rho_{cc}^{M}(\sigma)$ the contribution for a specific M value and an effective fluence $\sigma=P\tau_{\text{eff}}$. An integration was performed over the 800-kHz Doppler residue of the molecular beam. The result is included in Fig. 3(b) (dashed curves). Two conclusions can be drawn. The diminishing contrast for successive π pulses in case of a power scan and the better contrast in the time scan are well reproduced. The procedure to evaluate the measurements with the help of the averaged main value of $d_{ab}d_{bc}$ appears to be justified.

Concerning the two-color measurements a quantitative simulation was not attempted. The results shown in Fig. 8 show the right trend, but strong ac-Stark effects and interferences between individual transition pathways are likely to occur. Already, the comparison between the slopes of two-color excitation with Δ_1=70 MHz (Δ_2=82 MHz) and one-color excitation with Δ=76 MHz shows a deviation by more than a factor of 2 (see Figs. 4 and 8). For decreasing Δ_1 this effect becomes even more pronounced. In the dressed-state model it is easy to see that the presence of many photons in two radiation modes of different but nearly the same energy yields large multiplets of nearly degenerate states. The radiative coupling within these multiplets renders the dressed-state model untractable for quantitative discussions, and calculations should be based on the appropriate set of optical Bloch equations. Further discussions of multicolor multilevel excitation processes can be found elsewhere [9,30,31].

VI. CONCLUSIONS

Two-photon Rabi oscillations are demonstrated using one- and two-color excitation. For the one-color case the three-level system can be described in terms of the superposition of two states, equivalent to a two-level system, if a relatively large detuning of the intermediate level is assumed. From the number of π pulses the dipole strength can be recovered in good agreement with the theoretical value. For the two-color case the observed Rabi oscillations are

described only qualitatively. Multilevel couplings are likely to occur due to different interaction pathways involving different photons.

ACKNOWLEDGMENTS

The authors would like to thank C. Sikkens and F. van Rijn for their professional technical assistance. W. L. Meerts is acknowledged for his assistance with the computerized data acquisition. This work has been made possible through the financial support of the KUN, the NWO foundations STW and FOM, as well as the EC (network).

APPENDIX

The analytical formula for the population of the final level in a two-level system can be obtained from the optical Bloch equations (OBE). For the special case of a square pulse shape of the em field this results in an expression similar to Eq. (3). The interaction time τ results from the width of the square pulse divided by the beam velocity v. The strength of the em-field intensity is constant, which allows for analytical solution of the OBE.

For a Gaussian-field-intensity distribution the em-field strength experienced by the molecules varies in time, according to

$$\mathcal{E}(t)=\mathcal{E}_0 \exp\left[-\left(\frac{vt}{w_0}\right)^2\right] \tag{A1}$$

with ϵ_0 the maximum field strength, v the velocity of the beam molecules, and w_0 the half-width of the Gaussian profile. The OBE have to be solved with this time dependence of the em-field strength. Application of the pulse area theorem [19] gives the population ρ_{cc} for a laser field on resonance with the transition frequency as

$$\rho_{cc}=\sin^2\left[\left(\frac{d_{ab}d_{bc}}{2\hbar}\right)^2 \int \mathcal{E}^2(t)dt\right]. \tag{A2}$$

For a full Gaussian profile, time runs from $-\infty$ to ∞ and the integral can be solved analytically. When the Gaussian beam is partially cut off symmetrically around the center with a slit of total width $2a$ the integral can only be evaluated numerically. The effective interaction time for a two-photon transition is defined as

$$\tau_{\text{eff}}(a)=2\int_0^{a/v} \exp\left[-2\left(\frac{vt}{w_0}\right)^2\right]dt=\sqrt{\pi/2}\,\frac{w_0}{v}\,\text{Erf}\left(\frac{\sqrt{2}a}{w_0}\right), \tag{A3}$$

in which $\text{Erf}(x)$ is the error function [32]. This gives the effective interaction time with an unobstructed laser beam as

$$\tau_{\text{eff}}(a\to\infty)=\sqrt{\pi/2}\,\frac{w_0}{v}. \tag{A4}$$

This value can be compared to the interaction time with a square intensity profile, $2w_0/v$.

For the experiments it is necessary to know the magnitude of the electrical-field strength that results from the measured laser power. The relation between laser power and the local electrical-field strength is given by

$$P=\tfrac{1}{2}\epsilon_0 c\int_A \mathcal{E}^2(x,y)dA, \tag{A5}$$

for a laser field running in the $\hat{z}$ direction with electrical-field strength $\mathcal{E}(x,y)$ and with ϵ_0 the dielectric constant and c the speed of light. For a laser beam symmetrically cut off by a slit of total width $2a$ and using the general expression for a Gaussian beam the laser power is expressed by

$$P=2\epsilon_0 c w_0^2\mathcal{E}_0^2\int_0^a \exp\left[-2\left(\frac{x}{w_0}\right)^2\right]dx\int_0^\infty \exp\left[-2\left(\frac{y}{w_0}\right)^2\right]dy$$

$$=\frac{\pi}{4}\,\epsilon_0 c w_0^2\mathcal{E}_0^2\,\text{Erf}\left(\frac{\sqrt{2}a}{w_0}\right), \tag{A6}$$

where diffraction at the slit edges is neglected.

[1] C. Cohen-Tannoudji, J. Dupont-Roc, and G. Grynberg, *Atom-Photon Interactions* (Wiley, New York, 1993), Chap. VI.
[2] J. P. C. Kroon, H. A. Senhorst, H. C. W. Beijerinck, B. J. Verhaar, and N. F. Verster, Phys. Rev. A **31**, 3724 (1985).
[3] C. J. Bordé (unpublished).
[4] S. Avrillier, J.-M. Raimond, Ch. J. Bordé, D. Bassi, and G. Scoles, Opt. Commun. **39**, 311 (1981).
[5] B. Zhang, X. Gu, N. R. Isenor, and G. Scoles, Chem. Phys. **126**, 151 (1988).
[6] W. Q. Cai, T. E. Gough, X. J. Gu, N. R. Isenor, and G. Scoles, J. Mol. Spectrosc. **120**, 374 (1986).
[7] A. G. Adam, T. E. Gough, N. R. Isenor, and G. Scoles, Phys. Rev. A **32**, 1451 (1985).
[8] M. Gatzke, M. C. Baruch, R. B. Watkins, and T. F. Gallagher, Phys. Rev. A **48**, 4742 (1993).
[9] V. M. Akulin and N. V. Karlov, *Intense Resonant Interactions in Quantum Electronics* (Springer-Verlag, Berlin, 1992).
[10] J. Reuss and N. Dam, *Applied Laser Spectroscopy* (Plenum, New York, 1990), p. 227.
[11] B. W. Shore and J. Ackerhalt, Phys. Rev. A **15**, 1640 (1977).
[12] M. Sargent and P. Morowitz, Phys. Rev. A **13**, 1962 (1976).
[13] A. F. Linskens, N. Dam, J. Reuss, and B. Sartakov, Can. J. Phys. **72**, 1273 (1994).
[14] R. Loudon, *The Quantum Theory of Light* (Clarendon, Oxford, 1983), Chap. 2.
[15] B. W. Shore, *The Theory of Coherent Atomic Excitation* (Wiley, New York, 1990), Vol. 2, Chap. 13.
[16] V. N. Bagratashvili, V. S. Letokhov, A. A. Makarov, and E. A. Ryabov, *Multiple Photon Infrared Laser Photophysics and Photochemistry* (Harwood Academic, Chur, Switzerland, 1985), Chap. 3.
[17] M. D. Levenson and S. S. Kano, *Introduction to Nonlinear Laser Spectroscopy*, 2nd rev. ed. (Academic, San Diego, 1988), Chap. 2.
[18] P. F. Liao and J. E. Bjorkholm, Phys. Rev. Lett. **34**, 5 (1975).
[19] P. Meystre and M. Sargent III, *Elements of Quantum Optics*, 2nd ed. (Springer, Verlag, Berlin, 1991).

[20] A. F. Linskens, S. te Lintel Hekkert, and J. Reuss, Infrared Phys. **32**, 259 (1991).
[21] S. te Lintel Hekkert, A. F. Linskens, G. Pierre, B. G. Sartakov, and J. Reuss, Chem. Phys. **173**, 9 (1993).
[22] L. C. Bradley, K. L. Soohoo, and C. Freed, IEEE J. Quantum Electron. **QE-22** 234 (1986).
[23] S. te Lintel Hekkert, A. F. Linskens, I. Holleman, B. G. Sartakov, G. Pierre, and J. Reuss, Chem. Phys. **176**, 171 (1993).
[24] C. Liedenbaum, S. Stolte, and J. Reuss, Phys. Rep. **178**, 1 (1989).
[25] U. Gaubatz, P. Rudecki, S. Schiemann, and K. Bergmann, J. Chem. Phys. **92**, 5363 (1990).
[26] A. Linskens, Ph.D. thesis, University of Nijmegen, 1994 (unpublished).
[27] T. E. Gough, R. E. Miller, and G. Scoles, Appl. Phys. Lett. **30**, 338 (1977).
[28] A. F. Linskens, N. Dam, J. Reuss, and B. Sartakov, J. Chem. Phys. **101**, 9384 (1994).
[29] K. Kim, R. S. McDowell, and W. T. King, J. Chem. Phys. **73**, 36 (1980).
[30] G. K. Paramov, Chem. Phys. **177**, 169 (1993).
[31] S. S. Alimpiev and B. G. Sartakov, Laser Chem. **12**, 147 (1992).
[32] *Handbook of Mathematical Functions*, edited by M. Abramowitz and I. A. Stegun (Dover, New York, 1972).